ESCI upf. School of International Studies

Bachelor's Degree in Bioinformatics (UPF-UPC-UB)

Final Grade Project

Mapping the structural connectivity fingerprints of corticostriatal circuits in Huntington's Disease.

Irene Acero Pousa

Scientific director: Estela Càmara Mancha[1]

[1] IDIBELL, Cognition and Brain Plasticity Group.

Abstract

Huntington's disease (HD) is a genetic neurodegenerative disease caused by a mutation in the HTT gene which induces expansion of a cytosine-adenine-guanine (CAG) trinucleotide repeat. It involves a mixture of symptoms, including motor, cognitive and psychiatric deficits.

However, there is a high degree of heterogeneity in the prominence and evolution of each type of symptoms. The three main cortico-striatal circuits (motor, cognitive control and motivational) result affected by neurodegeneration beginning in the basal ganglia and extending to the cortices. One possible source of such interindividual differences among HD patients could be the variability in the degree of neurodegeneration of the different neural circuits. Interestingly, recent literature suggests that this variability in HD might be clusterized into distinct patterns of neurodegeneration associated with cognitive-motor and psychiatric profiles. The aim of this research is to characterize the structural connectivity of the three main cortico-striatal circuits in order to delineate specific neurodegeneration patterns that might underlay the different symptomatic profiles in HD.

We delineated the three main corticostriatal circuits including the motor, the associative and the limbic, each of them involving projections from different parts of the cortex to subparts of the striatum using probabilistic tractography implemented in Freesurfer with data collected from thirty-two HD gene carriers (15 premanifest and 17 manifest individuals) and thirty controls. Participants were scanned to obtain structural, microstructural and underwent neuropsychological evaluations. Then, the structural connectivity of the main tracts analyzed was used for a principal component analysis in order to distinguish specific neurodegeneration patterns. Finally, the loadings of extracted components were correlated with the symptomatic domains. We found differences in the structural connectivity pattern of the cortico-striatal circuits that was prominently associated with different symptoms. More severe cognitive signs were associated with a component consisting in a pattern of reduced structural connectivity in the three cortico-striatal networks, In contrast, depressive symptoms were correlated with the second component characterized by reduced structural connectivity in the associative circuit and increased connectivity in the limbic circuit. In conclusion, by delineating the structural connectivity of the main cortico-striatal circuits using a multivariate approach we were able to identify two different symptomatic profiles, one associated to cognitive features and the other associated to motivational signs, based on the underlying structural connectivity pattern. The importance of identifying different patterns of neurodegeneration could pave the way towards more personalized approaches tailored to the specific symptomatic profile of each individual.

Supplementary information: Supplementary data are available at GitHub link: https://github.com/Irenacero/FinalDegreeProject.git

1 Introduction

Huntington's disease (HD) is a dominant monogenic disease caused by an expansion of a cytosine-adenine-guanine (CAG) trinucleotide repeat in the exon 1 of the HTT gene, which leads to an abnormally long polyglutamine tract of the huntingtin (HTT) protein (Huntington and Others 1872).

HD involves a set of motor, cognitive and motivational disturbances (Harper 1996). Motor symptoms include chorea, which is being experienced by more than 90% of the patients and dystonia (Ross et al. 2014). Cognitive deficits manifest themselves more than 10 years before the patient receives a formal diagnosis and they include various deficits in executive functions such as planning, cognitive flexibility, cognitive inhibition or processing speed (Georgiou et al. 1995; Lawrence et al. 1996; Unschuld et al. 2013). Lastly, psychiatric symptoms involve apathy that almost all Huntington's patients experience at some point of the disease and depressive symptoms that were shown to be present especially in the premanifest stages of the disease (Julien et al. 2007).

Despite the monogenic nature of HD, there is a high degree of heterogeneity in the prominence and evolution of each type of symptoms, which means that they vary to a great extent across patients (Garcia-Gorro et al. 2019; Kim et al. 2015; Walker 2015; de Diego-Balaguer et al. 2016). Cognitive and motivational symptoms tend to appear before the patient receives a clinical diagnosis based on motor symptoms, and they can result in more pronounced disruptions compared to motor problems (Baquero and Martín 2015; Panza et al. 2010). Moreover, motivational symptoms are common in the disease but they are not seen in all patients (Walker 2015). As can be seen, there is a high abundance of interindividual differences in symptom prominence among HD patients.

One possible source of such interindividual differences among HD patients could be the variability in the degree of neurodegeneration of different neural circuits (Garcia-Gorro et al. 2019). In this regard, neuroimaging studies can contribute to the clustering of patients in different subgroups in order to implement more personalized treatments depending on the distinct neurobiological characteristics of each symptom (de Diego-Balaguer et al. 2016). Nevertheless, up to date, most of the studies in the field have focused on differences from healthy controls without considering the interindividual differences observed within the HD population. In some cases where they have been taken into account, it has been usually done in specific regions of interest based on a priori hypotheses (Kassubek et al. 2004; Rosas et al. 2006) or resulting from the main contrast between patients and controls (Harrington et al. 2014; Wolf et al. 2007). Moreover, although neuroimaging techniques are used widely to classify into different profiles patients with neurodegenerative, motivational and neurodevelopmental disorders (Costa Dias et al. 2015; Fair et al. 2012; Lubeiro et al. 2016; Park et al. 2017), their use in HD has not been very extensive.

To this end, recent studies were interested in the underlying neural substrates of different types of symptoms, for example, motor, cognitive and psychiatric, observed in HD patients (Garcia-Gorro et al. 2019). By combining clinical measures of the three types of symptoms and using a multivariate multimodal neuroimaging approach, they identified two distinct symptom profiles in HD that were characterized by different neural

substrates. They found a common neurobiological basis for cognitive and motor symptoms different from the one in the motivational domain. Further investigations revealed that more severe cognitive and motor symptoms were related to reduced grey matter, cortical thickness, and white matter integrity in networks related to the cognitive and motor functions. In contrast, psychiatric symptoms, namely depressive ones, were related to reduced cortical thickness in limbic and paralimbic regions. Moreover, cellular studies on post-mortem brain tissue of HD patients have found patterns of neuronal loss clusterized by motor, psychiatric and mixed (motor and psychiatric) profiles (Tippett et al. 2007; Thu et al. 2010; Nana et al. 2014; Mehrabi et al. 2016).

These pieces of evidence encourage the possibility that topological brain degeneration could underlie the phenotypic heterogeneity of HD. Different neuroimaging modalities have proven differential sensitivity to specific neural changes. Importantly, studies using resting-state functional MRI allow the identification of neural networks and the characterization of their connectivity. Indeed, a network-spread hypothesis has been proposed, suggesting that the progression of neurodegenerative diseases follows network structural connectivity. Research has shown that the striatum forms a hub and integrates motor, cognitive control and motivational circuits, which show a partial overlap and an interaction with each other. Specifically, there are three main corticostriatal circuits (Haber 2016). The motor circuit involves projections from the motor, premotor and sensorimotor areas to the putamen. The associative circuit, which is primary in executive functioning, involves dorsolateral and ventrolateral prefrontal cortex projections into the caudate. Lastly, the limbic circuit, which is involved in reward and emotional processing, consists of projections of orbitofrontal, ventromedial prefrontal and anterior cingulate cortices into the ventral striatum. Note that the degree of neurodegeneration in each of these circuits varies across HD patients. Using this information, we hypothesise that the structural connectivity between the cortex and the striatum is a predictor of the clinical profiles defined in previous research. Indeed, we expect to find two main patterns: a) a motor-cognitive profile, correlated with the caudate and putamen and b) a psychiatric profile, more connected with the accumbens.

2 Objectives

The aim of this research is to characterize the corticostriatal circuits in Huntington's Disease using fMRI data and to assess the structural connectivity signatures as a predictor of two clinical profiles previously defined. On the one hand, we expect to find a motor-cognitive profile and, on the other hand, a psychiatric profile.

3 Methods

3. 1 Participants

Thirty-two HD mutation carriers at different stages of the disease participated in the present study. Individuals were considered HD gene-carriers if they carried the HTT mutation with ≥ 39 CAG repeats. HD individuals were grouped into premanifest (N = 15) and manifest (N = 17) stages based on their Unified Huntington's Disease Rating Scale (UHDRS) diagnostic confidence score for motor abnormalities ("Unified Huntington's Disease Rating Scale: Reliability and Consistency" 1996), in which a score of four indicates manifest stage and a score less than four is considered as premanifest. However, we studied the disease as a continuum since the dichotomy between premanifest and manifest individuals is somewhat artificial (Ross et al. 2014) as it is based solely on the

basis of the motor dysfunction, but cognitive and psychiatric disturbances can occur before motor signs appear. None of the participants reported any neurological disorder other than HD.

Moreover, we included 30 controls matched for age ($t(70) = .13$, $p = .89$, two-tailed) and years of education ($t(70) = -.69$, $p = .48$, two-tailed), and with no history of psychiatric or neurological disorders.

This study was approved by the ethics committee of Bellvitge Institute for Biomedical Research (IDIBELL) and Bellvitge Hospital and all participants signed an informed consent to participate in it. All procedures followed were in accordance with the Helsinki Declaration of 1975.

3. 2 Symptom assessment

Each patient was assessed on the three symptom domains (motor, cognitive and psychiatric) using clinical scales and questionnaires. We used the UHDRS for the clinical assessment, a test that consists of motor, cognitive and behavioural subscales. Firstly, the motor symptoms were analyzed using the UHDRS motor score, with higher scores indicating more severe impairment. Secondly, the cognitive domain was evaluated looking cognitive flexibility (trail making test (TMT) B-A)(Tombaugh 2004), verbal fluency (phonemic letter fluency test FAS)(Butters et al. 1986), inhibitory control (Stroop interference)(Golden and Freshwater 1978), and psychomotor speed (symbol digit modalities test, SDMT)(Benedict et al. 2017). In this case, higher scores in the TMT B-A and Stroop interference, and lower scores in the verbal fluency and SDMT indicated poorer performance. Finally, psychiatric aspects included Depression and Anxiety subscales of the short version of the Problem Behavioural Assessment (PBA-s) (McNally et al. 2015), multiplying the frequency by severity, with more harsh symptoms indicated with higher scores. Some of the behavioural data in some participants were not collected due to time constraints.

3. 3 MRI data acquisition

MRI data were acquired through a 3T whole-body MRI scanner (Siemens Magnetom Trio; Hospital Clínic, Barcelona), equipped with a 32-channel phased array head coil. Structural images were assessed using conventional high-resolution 3D T1-weighted images, using a three-dimensional Magnetization Prepared Rapid Gradient Echo (MP- RAGE) sequence (repetition time (TR) = 1970 ms; echo time (TE) = 2.34 ms; inversion time (T1) = 1050 ms; flip angle = 9°; 1 mm isotropic voxels; 208 sagittal slices; matrix = 208 x 256 x 256; field of view (FOV) = 256 x 256 mm).

Diffusion-weighted MRI data were acquired using a dual spin-echo diffusion-tensor imaging sequence with GRAPPA (reduction factor of 4) cardiac gating, with echo time 92 milliseconds. Images were measured using 2 mm isotropic voxels, no gap, 60 axial slices, field of view 23.6 cm. In order to obtain the diffusion tensors, diffusion was measured along 64 non-collinear directions, using a single b-value of 1500 s/mm 2 interleaved with 9 non-diffusion (b = 0) images. To avoid chemical shift artefacts, frequency-selective fat saturation was used to suppress the fat signal.

3. 4 Preprocessing of DTI data

Diffusion-weighted images were automatically processed using FSL 5.0. More specifically, first head motion and eddy-current correction were performed using the FMRIB's Diffusion Toolbox in FMRIB's Software Library (FSL, http://www.fmrib.ox.ac.uk/fsl/fdt) and the gradient matrix was rotated accordingly (Leemans and Jones 2009). Second, the

diffusion tensor was then reconstructed using Diffusion Toolkit's least-squares estimation algorithm for each voxel provided in Diffusion Toolkit (http://www.trackvis.org/dtk) and its corresponding eigenvalues and eigenvectors were extracted to calculate the fractional anisotropy (FA), axial diffusivity (AD), radial diffusivity (RD) and apparent diffusion coefficient (ADC) maps.

Subsequently, local two-fibre orientation distributions were modelled in each voxel of the brain using the software module Bedpostx implemented in the FDT toolbox (Behrens et al. 2007). Probabilistic tractography was conducted in each participant's native diffusion space in order to delineate the fibre pathways between the respective seed and target regions by the inclusion of a midline exclusion mask and a cerebrospinal fluid mask (CSF) in transformed to native diffusion space. The midline hemisphere mask was created from the MNI152 1mm using FSL tools. CSF masks were created by the automatic segmentation of cerebrospinal fluid on the T1-weighted images using SPM (https://www.fil.ion.ucl.ac.uk/spm/software/spm12/). Probtrackx2 (Behrens et al. 2007) was run with the following settings (curvature threshold = 0.2, 5000 samples, 0.5mm step length, 2000 steps). For each subcortical region set as seed (caudate, putamen and accumbens) a bidirectional analysis was performed, initially from the subcortical seed to the selected cortical region, setting this as waypoint mask and, secondly, from the cortical area to the subcortical region, considered as termination mask. The mean image of these two analyses was computed as the final tract between the seed and target regions of the subject.

3. 5 Tractography dissections

In order to delineate the three main cortico-striatal circuits, we virtually dissected the caudate-executive frontal, putamen-motor, and the accumbens-limbic circuit.

For the virtual dissection of the different tracts, first, subcortical segmentation of the caudate, putamen and accumbens was performed bilaterally. Specifically, these regions were obtained after automated segmentation using the run_first_all script included in the FMRIB's Linear Image Registration Tool (FIRST) of the FMRIB Software Library (FSL) v5.0.9 (Mark Jenkinson et al. 2012) on the T1-weighted (T1w) image of each of the participants. Then, these ROIs were registered to the individual native diffusion space using the FSL FLIRT and FNIRT modules after normalizing both the structural T1 images and FA maps (M. Jenkinson and Smith 2001).

Second, the cortical target regions were defined using the FSL Harvard-Oxford Cortical Structural Atlas (Desikan et al. 2006) and consisted of the motor, the executive and the motivational areas. The motor network included the Precentral Gyrus; the executive network included the Middle, Superior and Inferior Frontal Gyrus and, finally, the motivational comprised the Anterior Cingulate Gyrus and the Frontal Orbital Cortex. The cortical regions were defined in the MNI space and were wrapped back to the individual native diffusion space using the inverse matrix transformation obtained using FSL FLIRT and FNIRT modules after normalizing the native FA maps.

Diffusion measures (FA, AD and RD) were extracted and averaged along the entire delineated tracts.

3. 6 Principal component analysis

Principal component analysis (PCA) (Fearn 2014) is a dimensionality reduction technique that allows the increase of interpretability of datasets and minimizes information loss. It creates new uncorrelated variables by

computing the data covariance matrix of the original data and, afterwards, performing eigenvalue decomposition on this matrix.

In the current study, PCA was performed combining the FA values of the six differential tracts, accumbens to motivational, caudate to executive and putamen to motor, left and right hemispheres each. Prior standardization to z-score of these values was computed.

3. 7 K-means clustering algorithm

K-means clustering is an unsupervised learning algorithm that divides the observations into k clusters, fixed a priori, in which each observation belongs to the cluster with the nearest mean.

In our case, we applied the algorithm with a k of 2 over the FA values of the distinct tracts. Again, data has previously been normalized to z-scores.

4 Results

4. 1 Probabilistic tractography paths

Probabilistic tractography was conducted in each participant's native diffusion space and three fibre pathways were delineated. First, a tract including accumbens as subcortical seed and motivational area as the cortical target region. Second, considering caudate as seed and executive region as target and, finally, a tract consisting of putamen area as seed and going to the motor cortex. Each of them was computed for the left and right hemispheres and diffusion measures were extracted, see Figure 1.

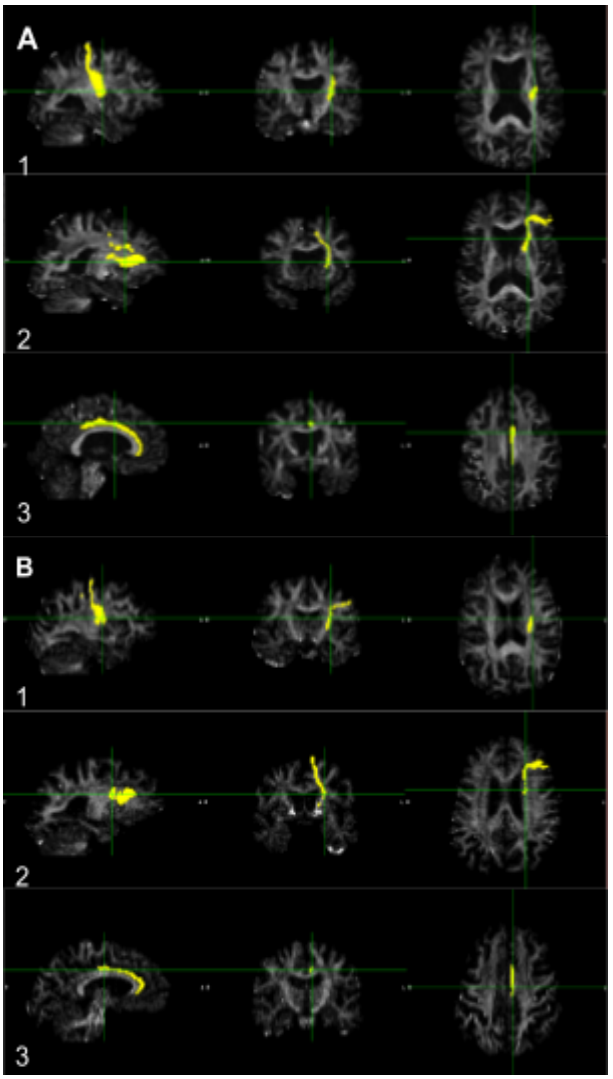

Fig. 1. Probabilistic fibre tracts delineated using Probtrackx2. 1 corresponds to putamen-motor tract, 2 to caudate-executive and 3 to accumbens-motivational. All images are thresholded at $p < 0.05$. (**A**) Images of a control subject. (**B**) Images of a patient subject.

4. 2 Principal Component Analysis

To identify different symptom profiles, scaled Principal Component Analysis (PCA) was conducted. From the initial six-dimensional factorisation, PCA provided a model with two main components accounting for 54.63% of the variance the first one (PC1) and 21.77% the second (PC2), see Figure 2. A third component with 15.07% was also distinguished, but it was discarded as it did not achieve the threshold of at least 20% of the

proportion of variance. These two components were a combination of the FA values of the six different probabilistic tracts. Loadings for the first principal component were all negative (Figure 3 A), indicating neurodegeneration in all tracts, while loadings for the second one had positive value in the accumbens-motivational tract, a negative value in the caudate-executive tract and approximately 0 value in the putamen-motor tract (Figure 3 B).

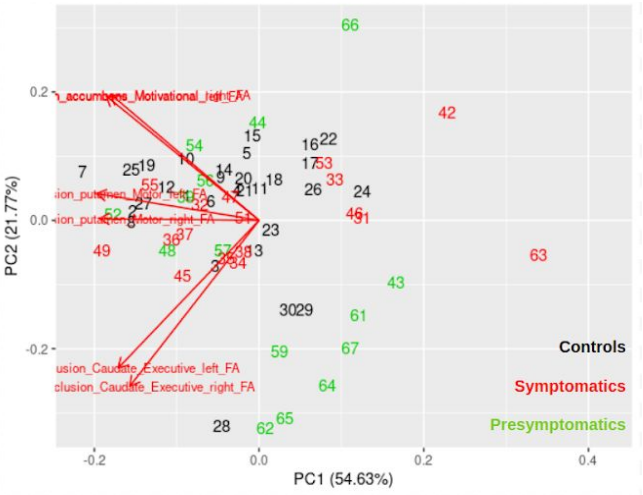

Fig 2. Representation of the first and second principal components. The numbering shows each subject being black the controls, red the symptomatics and green the presymptomatics. Loadings and percentage of variance explained by each component are also included.

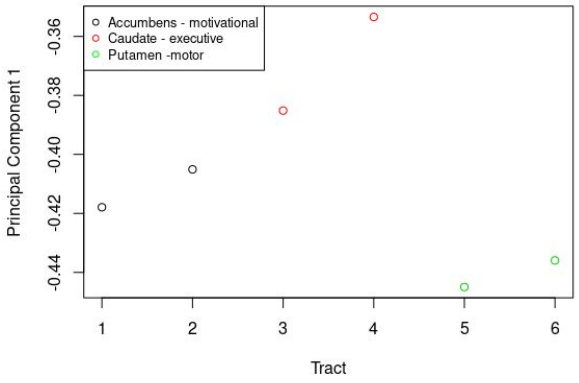

Fig 3 A. Loadings of PC1. Loadings are coloured by tract, black relates to the accumbens to motivational cortex path, red to the caudate to executive cortex and green to the putamen to motor cortex. PC1 loadings show negative values, corresponding to neurodegeneration in all tracts.

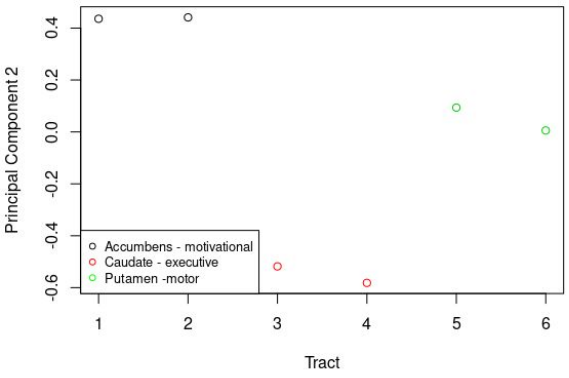

Fig 3 B. Loadings of PC2. Loadings are coloured by tract, black relates to the accumbens to motivational cortex path, red to the caudate to executive cortex and green to the putamen to motor cortex. Loadings for the accumbens to motivational path are positive, the ones for the caudate to executive are negative and, finally, for the putamen to motor remain neutral (approximately 0).

4. 3 K-means clustering algorithm

After scaling for z-score, FA values of the tracts were divided into two clusters of size 43 and 24 and overall performance of 34.1% using the k-means clustering algorithm. These were not responding to groups (Controls, Patients), as plot 2 in Figure 4 shows, but to the principal components computed in PCA, which can be seen in Figure 4 plot 3 and 4. This reaffirms the results obtained in the principal component analysis and discards the possibility of the two components indicating the differences between controls and patients.

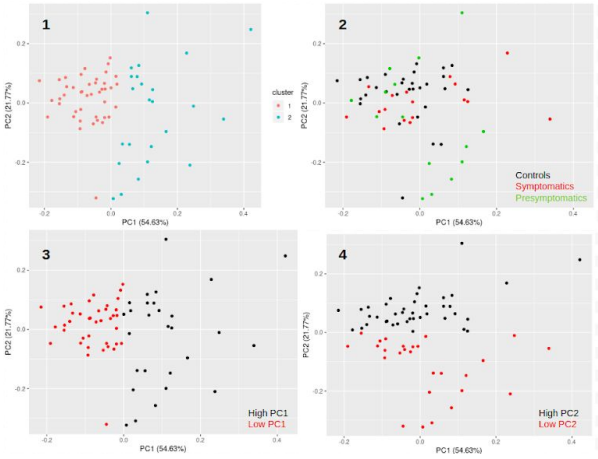

Fig 4. Clusters obtained using k-means

clustering algorithm. Colours in plot 1 represent the different clusters, whereas plot 2 is coloured by the subject's group, black associated with controls, red with symptomatics and green with presymptomatics. Plot 3 and 4 are coloured by low and high PC1 in the first case and low and high PC2 in the second one. Black shows high values and red low values in both of them.

4. 4 Relationship between neurodegeneration of the tracts and clinical measures

First and second principal components extracted from PCA were significantly correlated with some conductual measures. On the one hand, the subjects' loadings of PC1 showed to be significantly correlated with executive functions such as cognitive flexibility (TMT B-A: R = 0.61, $p < 0.01$) and suppression of interference (Stroop interference: R = -0.62, p = 0.0016), see Figure 5, green plots. In contrast, subjects' loading of the second principal component significantly correlated with depression scores (Depression score: R = -0.78, p = 0.0137), see Figure 5, grey plot. None of the components correlated significantly with motor variables.

These analyses suggest two distinct symptomatic profiles of Huntington's Disease patients. On the one hand, component 1 corresponds to a cognitive-executive profile and, on the other hand, component 2 corresponds to a psychiatric domain.

5 Discussion

The aim of the current study was to explore the structural connectivity patterns underlying the three main symptom domains of HD: motor, cognitive and psychiatric disturbances. Although the three of them characterize the disease, there is a high abundance of interindividual differences in symptom prominence and evolution among HD patients (de Diego-Balaguer et al. 2016). So far, recent studies were interested in the underlying neural substrates of different types of symptoms observed (Garcia-Gorro et al. 2019). This revealed two distinct symptom profiles which also differed in their neurobiological substrates. In other words, they found a common neurobiological basis for cognitive and motor symptoms different from the one in the psychiatric domain. Based on this study, we hypothesized that interindividual differences in structural connectivity patterns could also explain the variance seen in each symptom domain. We used MRI data that allowed us to study disease-related alterations in the cortico-striatal circuits affected in HD. Three main tracts were investigated according to the main cortico-striatal circuits, which were the motor, executive and motivational circuits and the seed regions defined were the putamen, the caudate and the accumbens.

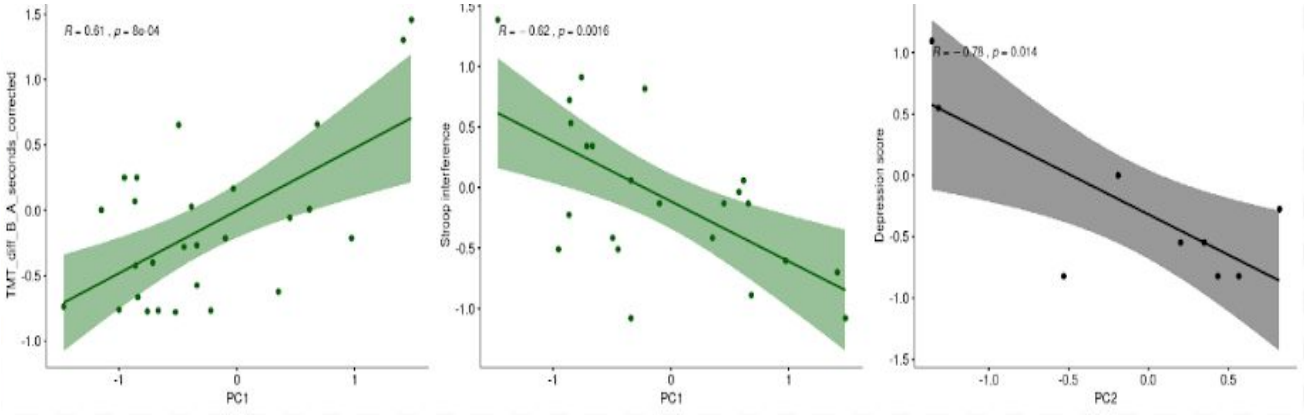

Fig 5. Relationship between subject loadings and conductual measures. Loadings of PC1 (in green) and PC2 (in grey) and cognitive flexibility, stroop interference and depression, in z-scores, from left to right. Correlation coefficients (R) and p-values (p) of each case are specified.

We obtained two main findings. On the one hand, we identified two different components across subjects based on the neurodegeneration values of the three tracts studied, two hemispheres each. These were found by conducting a principal component analysis. Moreover, clusterization of these variables was performed running k-means clustering algorithm for two clusters. Colouring the clusters obtained by different parameters (group of the subjects, first principal component and second principal component) concluded that the partition of these two clusters corresponded to the same division given by the PCA and not to a controls-patients or controls-presymptomatic-symptomatic distribution. These reaffirmed the components given by PCA, as the same results were obtained by two different analyses.

On the other hand, we related these two principal components with clinical measures. Correlation tests gave associations between the executive and cognitive variables (cognitive flexibility and suppression of interference) and PC1. In contrast, PC2 correlated with depression. With these findings, we identified two profiles relating neurodegeneration with symptoms in HD patients. Principal component 1 formed an executive-cognitive profile, whereas principal component 2 lead to a psychiatric profile. Patients in the first profile exhibited more severe executive and cognitive deficits and less severe motivational symptoms, while for the second profile this was contrarywise. This result is in line with Garcia-Gorro et al (2019), which identified a common neurobiological basis for motor and cognitive symptoms whereas the psychiatric domain was presenting a differentiated neural signature.

Moreover, loadings for PC1 were all negative, indicating neurodegeneration in all three tracts and for both hemispheres. Differently, loadings for the accumbens-motivational tract in PC2 showed to have positive values, whereas the caudate-executive path was negative and the putamen-motor resulted to be approximately 0. Although the need for further investigation in this point, these results could indicate a compensatory mechanism between the accumbens-motivational and the caudate-executive tracts in the second principal component.

In light of the above, using a dimensionality reduction approach on structural connectivity data we were able to identify two distinct profiles (cognitive and motivational). These results are interesting in clinical trials, as they could be used to define specific biomarkers for each symptom even before clinical signs appear. Moreover, the classification of patients would make trials more effective in time and resources, as new medicine would be tried in a better and more specific selection of patients. Moreover, having more homogenous groups would allow the development of more individualised treatments that target specific cognitive, executive and psychiatric alterations. This would also permit an increase of the understanding of the disease and its stages in each of the profiles, which would allow a better explanation of possible future steps to each patient and, hence, an improved psychological preparation.

6 Bibliography

Baquero, Miquel, and Nuria Martín. 2015. "Depressive Symptoms in Neurodegenerative Diseases." *World Journal of Clinical Cases* 3 (8): 682–93. https://doi.org/10.12998/wjcc.v3.i8.682.

Behrens, T. E. J., H. Johansen Berg, S. Jbabdi, M. F. S. Rushworth, and M. W. Woolrich. 2007. "Probabilistic Diffusion Tractography with Multiple Fibre Orientations: What Can We Gain?" *NeuroImage*.

https://doi.org/10.1016/j.neuroimage.2006.09.018.

Benedict, Ralph Hb, John DeLuca, Glenn Phillips, Nicholas LaRocca, Lynn D. Hudson, Richard Rudick, and Multiple Sclerosis Outcome Assessments Consortium. 2017. "Validity of the Symbol Digit Modalities Test as a Cognition Performance Outcome Measure for Multiple Sclerosis." *Multiple Sclerosis* 23 (5): 721–33. https://doi.org/10.1177/1352458517690821.

Butters, N., J. Wolfe, E. Granholm, and M. Martone. 1986. "An Assessment of Verbal Recall, Recognition and Fluency Abilities in Patients with Huntington's Disease." *Cortex; a Journal Devoted to the Study of the Nervous System and Behavior* 22 (1): 11–32. https://doi.org/10.1016/s0010-9452(86)80030-2.

Costa Dias, Taciana G., Swathi P. Iyer, Samuel D. Carpenter, Robert P. Cary, Vanessa B. Wilson, Suzanne H. Mitchell, Joel T. Nigg, and Damien A. Fair. 2015. "Characterizing Heterogeneity in Children with and without ADHD Based on Reward System Connectivity." *Developmental Cognitive Neuroscience* 11 (February): 155–74. https://doi.org/10.1016/j.dcn.2014.12.005.

Desikan, Rahul S., Florent Ségonne, Bruce Fischl, Brian T. Quinn, Bradford C. Dickerson, Deborah Blacker, Randy L. Buckner, et al. 2006. "An Automated Labeling System for Subdividing the Human Cerebral Cortex on MRI Scans into Gyral Based Regions of Interest." *NeuroImage* 31 (3): 968–80. https://doi.org/10.1016/j.neuroimage.2006.01.021.

Diego-Balaguer, Ruth de, Catherine Schramm, Isabelle Rebeix, Emmanuel Dupoux, Alexandra Durr, Alexis Brice, Perrine Charles, et al. 2016. "COMT Val158Met Polymorphism Modulates Huntington's Disease Progression." *PloS One* 11 (9): e0161106. https://doi.org/10.1371/journal.pone.0161106.

Fair, Damien A., Deepti Bathula, Molly A. Nikolas, and Joel T. Nigg. 2012. "Distinct Neuropsychological Subgroups in Typically Developing Youth Inform Heterogeneity in Children with ADHD." *Proceedings of the National Academy of Sciences of the United States of America* 109 (17): 6769–74. https://doi.org/10.1073/pnas.1115365109.

Fearn, Tom. 2014. "Probabilistic Principal Component Analysis." *NIR News*. https://doi.org/10.1255/nirn.1439.

Garcia-Gorro, Clara, Alberto Llera, Saul Martinez-Horta, Jesus Perez-Perez, Jaime Kulisevsky, Nadia Rodriguez-Dechicha, Irene Vaquer, et al. 2019. "Specific Patterns of Brain Alterations Underlie Distinct Clinical Profiles in Huntington's Disease." *NeuroImage. Clinical* 23 (June): 101900. https://doi.org/10.1016/j.nicl.2019.101900.

Georgiou, N., J. L. Bradshaw, J. G. Phillips, J. A. Bradshaw, and E. Chiu. 1995. "The Simon Effect and Attention Deficits in Gilles de La Tourette's Syndrome and Huntington's Disease." *Brain: A Journal of Neurology* 118 (Pt 5) (October): 1305–18. https://doi.org/10.1093/brain/118.5.1305.

Golden, Charles J., and Shawna M. Freshwater. 1978. "Stroop Color and Word Test." http://v-psyche.com/doc/Clinical%20Test/Stroop%20Color%20and%20Word%20Test.doc.

Haber, Suzanne N. 2016. "Corticostriatal Circuitry." *Dialogues in Clinical Neuroscience* 18 (1): 7–21. https://www.ncbi.nlm.nih.gov/pubmed/27069376.

Harper, Peter S. 1996. *Huntington's Disease*. Vol. 31. Bailliere Tindall.

Harrington, Deborah L., Dawei Liu, Megan M. Smith, James A. Mills, Jeffrey D. Long, Elizabeth H. Aylward, and Jane S. Paulsen. 2014. "Neuroanatomical Correlates of Cognitive Functioning in Prodromal Huntington Disease." *Brain and Behavior* 4 (1): 29–40. https://doi.org/10.1002/brb3.185.

Huntington, George, and Others. 1872. “On Chorea.” http://hdsa.org/wp-content/uploads/2017/08/On-Chorea.pdf.

Jenkinson, Mark, Christian F. Beckmann, Timothy E. J. Behrens, Mark W. Woolrich, and Stephen M. Smith. 2012. “FSL.” *NeuroImage*. https://doi.org/10.1016/j.neuroimage.2011.09.015.

Jenkinson, M., and S. Smith. 2001. “A Global Optimisation Method for Robust Affine Registration of Brain Images.” *Medical Image Analysis* 5 (2): 143–56. https://doi.org/10.1016/s1361-8415(01)00036-6.

Julien, Camille L., Jennifer C. Thompson, Sue Wild, Pamela Yardumian, Julie S. Snowden, Gwen Turner, and David Craufurd. 2007. “Psychiatric Disorders in Preclinical Huntington’s Disease.” *Journal of Neurology, Neurosurgery, and Psychiatry* 78 (9): 939–43. https://doi.org/10.1136/jnnp.2006.103309.

Kassubek, J., F. D. Juengling, T. Kioschies, K. Henkel, J. Karitzky, B. Kramer, D. Ecker, et al. 2004. “Topography of Cerebral Atrophy in Early Huntington’s Disease: A Voxel Based Morphometric MRI Study.” *Journal of Neurology, Neurosurgery, and Psychiatry* 75 (2): 213–20. https://www.ncbi.nlm.nih.gov/pubmed/14742591.

Kim, Ji-In, Jeffrey D. Long, James A. Mills, Elizabeth McCusker, Jane S. Paulsen, and PREDICT-HD Investigators and Coordinators of the Huntington Study Group. 2015. “Multivariate Clustering of Progression Profiles Reveals Different Depression Patterns in Prodromal Huntington Disease.” *Neuropsychology* 29 (6): 949–60. https://doi.org/10.1037/neu0000199.

Lawrence, A. D., B. J. Sahakian, J. R. Hodges, A. E. Rosser, K. W. Lange, and T. W. Robbins. 1996. “Executive and Mnemonic Functions in Early Huntington’s Disease.” *Brain: A Journal of Neurology* 119 (Pt 5) (October): 1633–45. https://doi.org/10.1093/brain/119.5.1633.

Leemans, A., and D. K. Jones. 2009. “Improved Model Fitting through Improved Eddy Current Distortion Correction in DTI.” *NeuroImage*. https://doi.org/10.1016/s1053-8119(09)70135-1.

Lubeiro, Alba, Cristina Rueda, Juan A. Hernández, Javier Sanz, Fernando Sarramea, and Vicente Molina. 2016. “Identification of Two Clusters within Schizophrenia with Different Structural, Functional and Clinical Characteristics.” *Progress in Neuro-Psychopharmacology & Biological Psychiatry* 64 (January): 79–86. https://doi.org/10.1016/j.pnpbp.2015.06.015.

McNally, George, Hugh Rickards, Mike Horton, and David Craufurd. 2015. “Exploring the Validity of the Short Version of the Problem Behaviours Assessment (PBA-S) for Huntington’s Disease: A Rasch Analysis.” *Journal of Huntington’s Disease*. https://doi.org/10.3233/jhd-150164.

Mehrabi, Nasim F., Henry J. Waldvogel, Lynette J. Tippett, Virginia M. Hogg, Beth J. Synek, and Richard L. M. Faull. 2016. “Symptom Heterogeneity in Huntington’s Disease Correlates with Neuronal Degeneration in the Cerebral Cortex.” *Neurobiology of Disease* 96 (December): 67–74. https://doi.org/10.1016/j.nbd.2016.08.015.

Nana, Alissa L., Eric H. Kim, Doris C. V. Thu, Dorothy E. Oorschot, Lynette J. Tippett, Virginia M. Hogg, Beth J. Synek, Richard Roxburgh, Henry J. Waldvogel, and Richard L. M. Faull. 2014. “Widespread Heterogeneous Neuronal Loss across the Cerebral Cortex in Huntington’s Disease.” *Journal of Huntington’s Disease* 3 (1): 45–64. https://doi.org/10.3233/JHD-140092.

Panza, Francesco, Vincenza Frisardi, Cristiano Capurso, Alessia D’Introno, Anna M. Colacicco, Bruno P. Imbimbo, Andrea Santamato, et al. 2010. “Late-Life Depression, Mild Cognitive Impairment,

and Dementia: Possible Continuum?" *The American Journal of Geriatric Psychiatry*. https://doi.org/10.1097/jgp.0b013e3181b0fa13.

Park, Jong-Yun, Han Kyu Na, Sungsoo Kim, Hyunwook Kim, Hee Jin Kim, Sang Won Seo, Duk L. Na, Cheol E. Han, Joon-Kyung Seong, and Alzheimer's Disease Neuroimaging Initiative. 2017. "Robust Identification of Alzheimer's Disease Subtypes Based on Cortical Atrophy Patterns." *Scientific Reports* 7 (March): 43270. https://doi.org/10.1038/srep43270.

Rosas, H. Diana, David S. Tuch, Nathanael D. Hevelone, Alexandra K. Zaleta, Mark Vangel, Steven M. Hersch, and David H. Salat. 2006. "Diffusion Tensor Imaging in Presymptomatic and Early Huntington's Disease: Selective White Matter Pathology and Its Relationship to Clinical Measures." *Movement Disorders: Official Journal of the Movement Disorder Society* 21 (9): 1317–25. https://doi.org/10.1002/mds.20979.

Ross, Christopher A., Elizabeth H. Aylward, Edward J. Wild, Douglas R. Langbehn, Jeffrey D. Long, John H. Warner, Rachael I. Scahill, et al. 2014. "Huntington Disease: Natural History, Biomarkers and Prospects for Therapeutics." *Nature Reviews. Neurology* 10 (4): 204–16. https://doi.org/10.1038/nrneurol.2014.24.

Thu, Doris C. V., Dorothy E. Oorschot, Lynette J. Tippett, Alissa L. Nana, Virginia M. Hogg, Beth J. Synek, Ruth Luthi-Carter, Henry J. Waldvogel, and Richard L. M. Faull. 2010. "Cell Loss in the Motor and Cingulate Cortex Correlates with Symptomatology in Huntington's Disease." *Brain: A Journal of Neurology* 133 (Pt 4): 1094–1110. https://doi.org/10.1093/brain/awq047.

Tippett, Lynette J., Henry J. Waldvogel, Sally J. Thomas, Virginia M. Hogg, Willeke van Roon-Mom, Beth J. Synek, Ann M. Graybiel, and Richard L. M. Faull. 2007. "Striosomes and Mood Dysfunction in Huntington's Disease." *Brain: A Journal of Neurology* 130 (Pt 1): 206–21. https://doi.org/10.1093/brain/awl243.

Tombaugh, Tom N. 2004. "Trail Making Test A and B: Normative Data Stratified by Age and Education." *Archives of Clinical Neuropsychology: The Official Journal of the National Academy of Neuropsychologists* 19 (2): 203–14. https://doi.org/10.1016/S0887-6177(03)00039-8.

"Unified Huntington's Disease Rating Scale: Reliability and Consistency." 1996. *Movement Disorders*. https://doi.org/10.1002/mds.870110204.

Unschuld, Paul G., Xinyang Liu, Megan Shanahan, Russell L. Margolis, Susan S. Bassett, Jason Brandt, David J. Schretlen, et al. 2013. "Prefrontal Executive Function Associated Coupling Relates to Huntington's Disease Stage." *Cortex; a Journal Devoted to the Study of the Nervous System and Behavior* 49 (10): 2661–73. https://doi.org/10.1016/j.cortex.2013.05.015.

Walker, Ruth H. 2015. "Management of Neuroacanthocytosis Syndromes." *Tremor and Other Hyperkinetic Movements* 5 (October): 346. https://doi.org/10.7916/D8W66K48.

Wolf, Robert Christian, Nenad Vasic, Carlos Schönfeldt-Lecuona, G. Bernhard Landwehrmeyer, and Daniel Ecker. 2007. "Dorsolateral Prefrontal Cortex Dysfunction in Presymptomatic Huntington's Disease: Evidence from Event-Related fMRI." *Brain: A Journal of Neurology* 130 (Pt 11): 2845–57. https://doi.org/10.1093/brain/awm210.